Ordered Ferroelectric PVDF−TrFE Thin Films by High Throughput Epitaxy for Nonvolatile Polymer Memory

Youn Jung Park,[†] Seok Ju Kang,[†] Bernard Lotz,[‡] Martin Brinkmann,[‡] Annette Thierry,[‡] Kap Jin Kim,[§] and Cheolmin Park*,[†]

Department of Materials Science and Engineering, Yonsei University, Seoul, Korea, Institut Charles Sadron 23, Rue du Loess, Strasbourg 67034, France, and College of Environment and Applied Chemistry, Department of Advanced Polymer and Fiber Materials, Kyung Hee University, Yongin-si, Gyeonggi-do 449-701, Korea

Received July 5, 2008; Revised Manuscript Received September 13, 2008

ABSTRACT: High throughput epitaxy of a thin ferroelectric poly(vinylidene fluoride-*co*-trifluoroethylene) (PVDF−TrFE) film is demonstrated on a molecularly ordered poly(tetrafluoroethylene) (PTFE) substrate based on spin coating method over the area of a few centimeter square. The lattice match between $(010)_{PVDF-TrFE}$ and $(100)_{PTFE}$ results in *b* and *c* axes of PVDF−TrFE crystals preferentially parallel to *a* and *c* of PTFE, respectively and consequently produces global ordering of the edge-on PVDF−TrFE crystalline lamellae aligned perpendicular to the rubbing direction of PTFE, its *c*-axis. The epitaxially grown PVDF−TrFE film is successfully incorporated for arrays of ferroelectric capacitors that exhibit not only the significant reduction of ferroelectric thermal hysteresis but also the descent remanent polarization at very low effective operating voltage of ±5 V maintained to 88% of its initial value after number of fatigue cycles of 5×10^8 in the mode of bipolar pulse switching. A ferroelectric field effect transistor memory with epitaxially grown PVDF−TrFE layer as gate dielectric shows the saturated *I*−*V* hysteresis with bistable on/off ratio of approximately 10^2.

Introduction

Information storage devices of ferroelectric polymers such as poly(vinylidene fluoride) (PVDF) and its copolymers with trifluoroethylene (TrFE) have been of a great attention in virtue of mainly low cost solution processibility based on spin coating for their potential use in nonvolatile memory technology, one of the most essential technologies in the current mobile industry.[1−4] The basic ferroelectric polymer storage element is metal/ferroelectric polymer/metal (MFM) capacitor in which a ferroelectric polymer thin film sandwiched between arrays of metal electrodes that makes possible electrical charge signaling across the structure. More recently ferroelectric thin films have been applied as gate dielectric to form a ferroelectric field-effect transistor (FeFET) device structure. The polarization state of the ferroelectric gate set by the polarity of the writing gate voltage controls the electrical conductance of the channel between source and drain electrode.[5,6]

Since the minimum electric field:coercive field required for PVDF and PVDF−TrFE is high and approximately 50 MV/m, the films must be as thin as possible in order to reduce the applied voltage. The polarization behavior strongly influenced by the crystallinity of PVDF−TrFE film below its Curie temperature abruptly decreases when the film thickness reaches less than 100nm due to the significant reduction of the degree of crystallization of the film.[7,8] Effective *b* axis orientation of ferroelectric PVDF−TrFE crystal parallel to electric field is also of a prime importance for successful device performance. The abrupt reduction of polarization in spin cast thin PVDF−TrFE films has been observed not only with decrease of film thickness[9] but also upon melting and recrystallization.[10] The crystal orientation dependent polarization was also investigated in Al/PVDF−TrFE/Au capacitors in which Au bottom electrode was treated with self-assembled monolayers for controlling chemical nature of surface. [11] In general a preferred crystal orientation observed on surfaces with polar nature is found to provide good polarization.

Full utilization of ferroelectric properties of PVDF−TrFE thin films can be therefore achieved by maximizing the degree of crystallinity with the effective orientation of the crystals with respect to electric field. In spite of numerous previous studies for controlling both structure and orientation of PVDF and PVDF−TrFE crystals including melt drawing,[12] quenching,[13−15] thermal gradient and solvent evaporation, and so on,[16−18] a monolithic single crystal preferentially grown on a metal electrode surface would be the best for the purpose by using the epitaxial crystallization of ferroelectric materials. The recent advances in synthesis of epitaxial pervoskite ferroelectrics are promising on silicon.[19−22] Inorganic epitaxial ferroelectric films have been deposited on various appropriate single crystal substrates. For example, a carefully controlled MOCVD process has been widely utilized for fabricating epitaxial films of PZT, SBT, BLT, and BNT for different orientations which exhibit the properties very similar to those expected for bulk single crystals with square hysteresis loops and low coercive fields.[21,22]

The epitaxial crystallization of polymers has been accomplished on various substrates including inorganic substrates (e.g., alkali halides), and organic substrates such as benzoic acid and anthracene and so on.[23,24] We also employed the concept of epitaxy to self-assembled block copolymers with benzoic acid for controlling their nanostructures.[25] From the industrial point of view, however, the polymer epitaxy has two main critical issues. First, both inorganic and organic surfaces appropriate for epitaxy are hardly formed on a metallic bottom electrode substrate and in particular organic surfaces are usually very inhomogeneous, rendering it difficult to make flat surface in large scale for device fabrication. Second, in most cases, the spin coating technique, one of the most desirable film formation process in current industry, is hardly applicable for depositing polymer films by epitaxy.

* Corresponding author. Telephone: 02-2123-2833. Fax: 02-312-5375. E-mail: cmpark@yonsei.ac.kr.
[†] Department of Materials Science and Engineering, Yonsei University.
[‡] Institut Charles Sadron.
[§] College of Environment and Applied Chemistry, Department of Advanced Polymer and Fiber Materials, Kyung Hee University.

10.1021/ma801495k CCC: $40.75
Published on Web 10/29/2008

A process was developed by Wittmann and Smith to create flat and smooth poly(tetrafluoroethylene) (PTFE) substrates. [26] The method was based on fabrication thin polymer films on substrates by the friction force generated while a heated PTFE bar was slowly moved under pressure over a substrate. Molecularly arranged polymer chains well aligned along the moving direction acted as single crystal surface on which various polymers were epitaxially grown. [27] We envisioned robust epitaxy of PVDF−TrFE on a textured PTFE single crystal surface due to the similar chemical constituents of both polymers as well as the crystallographic matching of the two polymers. Here we present the epitaxy of thin PVDF−TrFE films on molecularly ordered PTFE surface by *spin coating* and subsequent thermal annealing. Nearly single crystalline polymer films were obtained with *a* axis of PVDF−TrFE crystals aligned parallel to the PTFE surface normal, giving rise to the crystalline lamellae directionally oriented perpendicular to the chain axis of PTFE. Furthermore, the facile formation of uniform single crystal PTFE surface on a metallic substrate in very large area allowed us to fabricate not only arrays of ferroelectric capacitors but also FeFET with the epitaxially grown PVDF−TrFE thin film.

Experimental Section

Epitaxy of PVDF−TrFE. A molecularly ordered thin PTFE layer was produced as follows. First, cleaning was done for the glass substrates (Corning 2147) by the method commonly used to the ITO. The cleaning process started with (1) ultrasonication in acetone and ethanol for 10 min, (2) a soft nylon brush was used to do soft mechanical scrubbing, and (3) the glass was rinsed with Milli-Q water. On these cleaned glass substrates, PTFE films are prepared by the friction-transferred process, the method by sliding a PTFE rod, as described elsewhere.[26] PTFE thin films were coated on the substrates by pressing a rod of PTFE ($\sim 1.5 \times 10^6$ Pa) and sliding it against the glass with the rate of 0.2 mm/s, at the temperature of the glass of approximately 300∼315 °C. The friction transferred PTFE film is approximately 25−30 nm thick, and the polymer chains are arranged parallel to the sliding direction.

PVDF−TrFE copolymer with 27.5 wt % TrFE kindly supplied from MSI Sensors, PA, USA was spin coated on the oriented PTFE prepared by the friction-transferred method. The melting (T_m) and Curie (T_c) temperatures of PVDF−TrFE were 150 and 80 °C, respectively. Thin film formation was done by spin coating of 1 wt% PVDF−TrFE solution in methyl ethyl ketone (MEK) with 2000∼3000 rpm for 60 s. Heat treatments for the films were performed on the heating stage (Linkam 600, U.K.) at 135 °C for 2 h.

Structure Characterization. The morphologies of crystalline polymer films were examined in the electron microscopy (Philips CM12) under bright field and selected area diffraction at 120 kV. In order to analyze molecular structure in detail, we investigated thin films of bilayers of PVDF−TrFE/PTFE by electron diffraction. For preparation of TEM samples, bilayer films are coated with carbon film, then stripped off from the glass substrates and transferred to copper grids with the help of poly(acrylic acid). We also performed grazing-incidence X-ray diffraction (GIXD) for structure analysis,[28] on the 4C2 beam line at the Pohang Accelerator Laboratory in Korea. The samples were mounted on an *X* and *Y* axes goniometer. The scattered beam intensity was recorded with an SCX:4300-165/2 CCD detector (Princeton Instruments). 2D GIXD patterns were obtained in the range $0 < q_z < 2.33$ Å^{-1}, $0 < q_{xy} < 2.33$ Å^{-1} ($q = 4\pi(\sin\theta)/\lambda$, with *Z* perpendicular and *XY* parallel to the substrate) with the monochromatized X-rays ($\lambda =$ 0.13807 nm) under vacuum.

Ferroelectric Properties. Friction-transferred PTFE films were deposited as described above on Au sputtered Silicon substrate, followed by epitaxial crystallization of PVDF−TrFE layer. Ferroelectric polymer capacitors were fabricated to measure polarization hysteresis loop. Aluminum top electrodes were evaporated on polymer films using a shadow mask with holes of 200 μm in diameter under pressure of $\sim 10^{-6}$ mB and at a rate of ∼0.1 nm/s. Ferroelectric properties were obtained using a virtual ground circuit (Radiant Technologies Precision LC unit) and fatigue measurement was performed by applying bipolar pulse train with the driving voltage of 20 V and stress frequency of 10 000 Hz. A FeFET was made with Au substrate as the bottom gate on which a PVDF–TrFE film was spin coated on a friction-transferred PTFE layer. A pentacene was thermally evaporated under a pressure of 10^{-6} mB and at a rate of 0.1−0.2 Å/s. Source/drain Au films were sequentially patterned on pentacene through shadow mask on the substrate at room temperature by thermal evaporation in a vacuum chamber with the deposition rates of 1 Å/s. The pentacene and the Au films were 60 and 100 nm thick, respectively. In addition, the electrical properties of the devices were measured using semiconductor systems (E5270B, HP4284A, Agilent Technologies). All measurements were done in a dark box at room temperature.

Results and Discussion

Highly ordered thin films of PVDF−TrFE by epitaxial crystallization on PTFE substrates were visualized by bright field TEM in Figure 1b. Edge-on crystalline lamellae on the bottom PTFE surface with the thickness ranging from 20 to 30 nm were aligned normal to the rubbing direction with which thin PTFE layered crystal is fabricated. The periodic arrays of crystalline lamellae are also confirmed by the fast Fourier transform (FFT) of the TEM image with the spot-like first order reflection in the inset of Figure 1b. The friction process for thin PTFE film frequently produces the bundles of PTFE chains aggregated with each other on which the film partially becomes thicker as characterized with the darker contrast in the right bottom of Figure 1b. The difference between two regions is approximately 10 nm in height and even on the bundles of PTFEs well defined ordering of PVDF−TrFE crystals occurs with a few of film defects arising from mechanical tearing of the film in Figure 1b. The observed alignment of ferroelectric polymer crystal lamellae on the PTFE surface is clearly distinguishable from the disordered needle-like crystalline lamellae which we produced with all the same process but the PTFE substrates. The characteristic crystalline lamellae are randomly oriented PVDF−TrFE crystal, approximately 20 and 400 nm in width and length, respectively, as shown in Figure 1a.

The selected area diffraction (SAD) in TEM was utilized to investigate the molecular orientation of the ordered PVDF−TrFE crystalline lamellae formed on a PTFE crystal surface as shown in Figure 1c and d. A combined diffraction pattern of both the oriented PVDF−TrFE and PTFE obtained in Figure 1c enables us conveniently to determine the molecular ordering of PVDF−TrFE epitaxially formed with respect to PTFE surface. A single crystal-like texture of the rubbed PTFE is well characterized with the series of spot-like reflections corresponding to ones from *ac* plane of PTFE crystals. As indexed in the SAD pattern, in particular a strong reflection on the meridian arises from $(0\ 0\ 15)_{PTFE}$ whose direction is parallel to the helix axis of PTFE chains, i.e. the rubbing direction. The representative reflection from PVDF−TrFE is observed near 2.55 Å on the meridian which corresponds to $(0\ 0\ 1)_{PVDF-TrFE}$ (Figure 1c). The results from the meridian reflections from both polymers, therefore, indicate that PVDF−TrFE crystal is lined up with its *c*-axis parallel to the helical chain axis of PTFE substrates.

Here, it is required to summarize the crystal structure of PVDF−TrFE with respect to the ferroelectric phase transition.[29−31] There are three different crystalline phases reported: (1) the ferroelectric low-temperature phase (LP), (2) the paraelectric high-temperature phase (HP), and (3) the cooled phase (CP). The ferroelectric LP consists of planar zigzag chains with the lattice constants as follows: $a = 9.12$ Å, $b = 5.25$ Å, $c = 2.55$ Å ($\beta = 93^o$). The HP, which appears above the phase

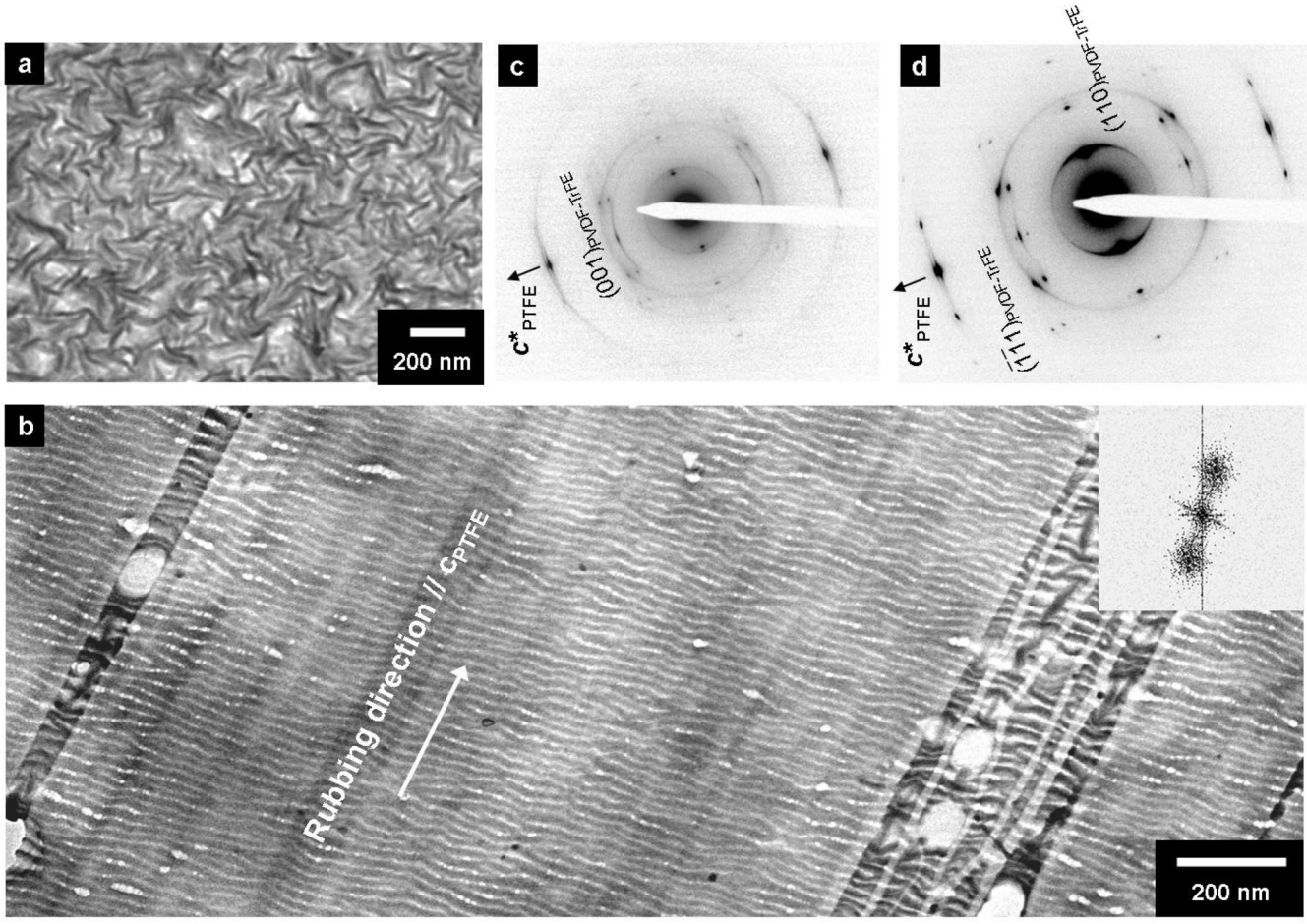

Figure 1. Bright field TEM micrographs of (a) a thin PVDF−TrFE film spin coated and annealed at 135 °C on a silicon substrate with the characteristic needle-like crystalline lamellae having approximately 20 and 400 nm in width and length and (b) a PVDF−TrFE film highly oriented by epitaxial crystallization on friction transferred PTFE substrates. The white arrow indicates a chain axis of PTFE parallel to the rubbing direction. The aligned edge-on lamellae of PVDF−TrFE uniformly cover most surfaces. An inset of part b corresponds to a fast Fourier transform (FFT). SAD patterns of PVDF−TrFE/PTFE layered film with the specimen (c) at normal incidence and (d) tilted by 30° around meridian show that the *c* and *a* axis of PVDF−TrFE crystals are parallel to *c* and *b* axis of PTFE, respectively.

transition temperature T_c, has hexagonal crystal packing ($a = b = 5.63$ Å, $c = 4.60$ Å) with the molecular chains of a disordered conformation, $T_3GT_3\bar{G}$, $T\bar{G}$, leading to the nonpolar characteristic. The crystal structure of CP ($a = 9.16$ Å, $b = 5.43$ Å, $c = 2.53$ Å, $\beta = 93°$) is similar to that of LP, but the zigzag chains tilt by about 18°. The phase transitions from LP to HP through CP and vice versa were observed during the heating and cooling process, but the transition behavior depends on the VDF molar fraction. Increasing VDF molar ratio of >65%, only LP appears at room temperature. Therefore, the ferroelectric copolymer, we used in this study, is VDF 72% copolymer with TrFE and has mostly LP at room temperature after the additional annealing procedure.

At the equator, on the other hand, the series of strong (*h*00) reflections of PTFE are apparent with a *weak* diffraction peak from PVDF−TrFE close to the $(100)_{PTFE}$ detected at the spacing of 4.48 Å in Figure 1c. The reflection arises from either (110) or (200) of PVDF−TrFE crystals, based on the fact that the β PVDF−TrFE crystal phase has a pseudo hexagonal orthorhombic lattice which is characterized by a $\sqrt{3}/2$ ratio of its *a* and *b* axes and in turn leads to nearly equal (200) and (110) spacings. In order to discern PVDF−TrFE crystal diffraction peak, the samples were tilted by approximately 30° from their original position around meridian as shown in Figure 1d. One can notice that the diffracted peak from either (110) or (200) is more intensified and the additional reflection as indicated with an arrow is observed near 2.12 Å which can result from either $(\bar{1}\bar{1}1)$ or $(\bar{2}01)$ paired with the intensified reflection of (110) or (200), respectively. As we noted ahead, the molecular conformation of PVDF−TrFE at the room temperature is influenced by the VDF content in the copolymer. It has been found that the copolymer with the higher VDF content (>65%), which also corresponds to the sample we used, exhibits mostly planar zigzag (*all-trans*) conformation, regardless of regioregularity.[30,31] That is, PVDF−TrFE with large amount of VDF has a crystal structure similar to that of β-PVDF in spite of the difference in lattice dimensions of the two polymers, which enables us to scrutinize the crystal structure of PVDF−TrFE based on that of PVDF β phase presented in the *Cerius* software.[32] On the basis of the fact that the reflection from $(\bar{2}01)$ is supposed to be absent in an idealized PVDF−TrFE crystal structure[32] we can index two reflections with (110) and $(\bar{1}\bar{1}1)$. The SAD analysis combined with the tilting experiment revealed the molecular structure of the ordered PVDF−TrFE crystals on PTFE surface in which the $bc_{PVDF-TrFE}$ plane is preferentially in contacts with *ac* plane of PTFE substrate. Well-ordered PVDF−TrFE edge-on lamellae are therefore aligned perpendicular to the chain axis, *c*-axis with the *a*-axis parallel to the surface normal. The comparison of the crystallographic lattices of two contact planes suggests a possible epitaxy of PVDF−TrFE on PTFE in terms of matching the PVDF−TrFE interchain distance of the $b_{PVDF-TrFE}$ periodicity (5.25 Å) with the *a* periodicity of the PTFE unit cell (5.66 Å) with the lattice mismatching ratio of 7.2%. It is noteworthy that the (110) reflection vaguely appearing

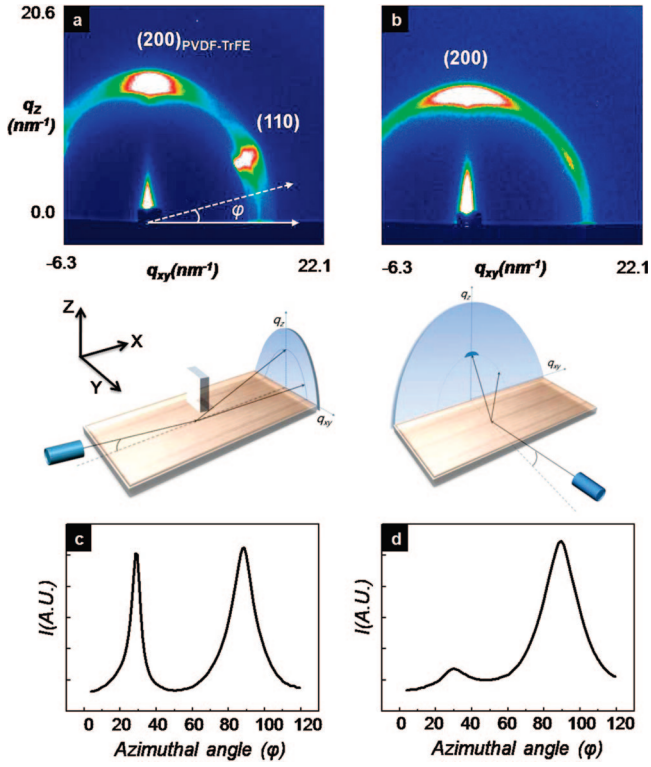

Figure 2. 2D GIXD patterns of PVDF−TrFE/PTFE bilayered films with two different incident beam along (a) *X* and (b) *Y* directions. The sample geometries with respect to X-ray beam for (a) and (b) are shown in the schematics below. (c and d) Equitorial azimuthal intensity profiles of parts a and b, respectively, as a function of scanning azimuthal angle, ϕ indicated with the arrow in part a. With the beam parallel to *X* axis, two strong reflections from (200) and (110) are equivalent in the intensity. By comparison, (200) peak is dominantly detected when the rubbing direction of the sample is normal to the beam.

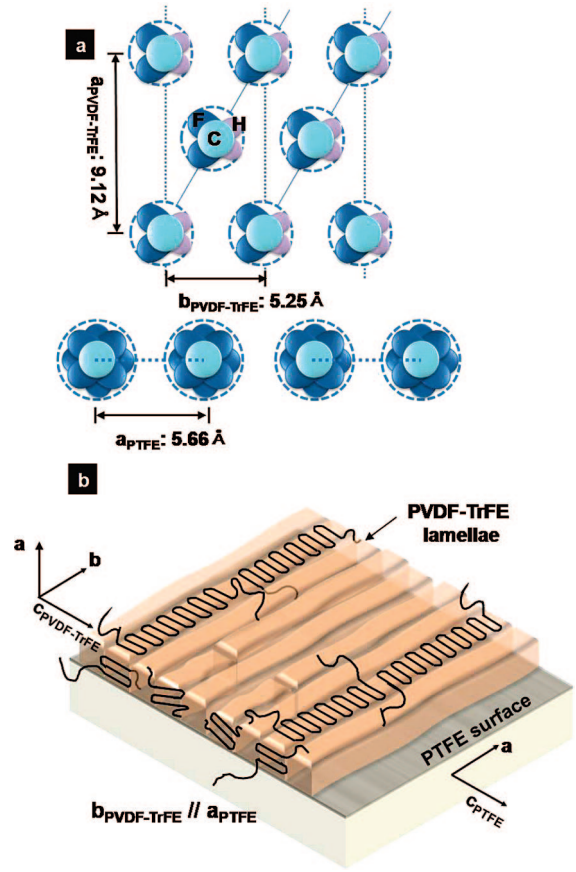

Figure 3. Schematic representation of (a) molecular and (b) microstructual orientation of PVDF−TrFE thin film epitaxially grown on PTFE surface. PVDF−TrFE/PTFE interface at the contact surface is seen along the chain axes in part a. The $bc_{\text{PVDF-TrFE}}$ plane is in contact with the ac_{PTFE} plane with the epitaxial relation of $b_{\text{PVDF-TrFE}}//a_{\text{PTFE}}$. The crystalline lamellae of PVDF−TrFE are aligned perpendicular to the chain axis of PTFE, rubbing direction of PTFE substrate in part b. Some defects with different oriented lamellae are also shown in the schematic.

in Figure 1c is supposed to be completely suppressed due to the *bc* plane eptiaxy of PVDF−TrFE on PTFE unless there exist some misaligned crystalline lamellae.

Further study on the oriented PVDF−TrFE on PTFE substrate was performed with the Grazing Incidence X-ray diffraction (GIXD) experiment which allowed us to investigate the X-ray scattering from the cross-sectional planes of the oriented film. We defined that the PTFE rubbing direction corresponds to *X*, the neutral direction to *Y*, and the through thickness direction to *Z* as schematically depicted in Figure 2a. The anisotropy in the diffraction patterns demonstrated in Figure 2a and b explains the existence of crystalline edge-on lamellae stacked along the one direction on rubbed PTFE surface. A 2D GIXD pattern with the incident X-ray beam parallel to the rubbing direction of PTFE, i.e. the *YZ* plane normal presents two strong reflections on the meridian and the 30° away from the horizontal. Since the previous SAD pattern analysis indicates the epitaxy of the *bc* plane of PVDF−TrFE crystals on *ac* plane of PTFE, we can expect (*hk*0) reflections of PVDF−TrFE with the X-ray beam parallel to the helix axis of PTFE, i.e., the chain *c*-axis of PVDF−TrFE. The two diffractions observed in Figure 2a are therefore indexed as (200) and (110) for the meridian and off-meridian one, respectively. The azimuthal intensity profile of Figure 2a exhibits the two diffractions with almost equal intensity, implying a 6-fold hexagonal symmetry of the epitaxially grown PVDF−TrFE crystals (Figure 2c). The degree of orientation of the two diffractions are, however, different with the greater full width half-maximum (fwhm) value of (200) peak ($\sim$ 30°) due to the denser crystal packing along (110) direction than (100) one in PVDF−TrFE crystals along the surface normal of the epitaxial film. It is noted that the degree of crystallization of an epitaxially grown PVDF−TrFE film is approximately 70%, calculated from the GIXD results and almost similar to that of a film spin coated and subsequently annealed at 135 °C for 2 h on a Si substrate.[10]

In comparison, the reflection from (110) is nearly absent when the sample is rotated with 90° and the beam is now perpendicular to *XZ* plane because only (*h*0*l*) reflections of PVDF−TrFE are allowed in the condition. The diffraction obtained in Figure 2b therefore corresponds to (200) and the diffraction intensity profile with the azimuthal angle shown in Figure 2d supports our argument with the intensity of the off-meridian diffraction at 30 ° significantly lower than that at 90°. It should be noted that fwhm of the (200) reflection in Figure 2c is smaller than that in Figure 2d, which confirms the better orientation along the *b* axis of PVDF−TrFE crystals mainly due to the stronger structural correlation arising from the eptiaxy. In fact the weaker interaction along the chain axis between two crystals gave rise to the crystalline PVDF−TrFE lamellae which tend to orient with the slight fluctuation as clearly evidenced in Figure 1b.

Both electron microscopy and X-ray diffraction experiment with different incident beam directions enabled us to conclude that the single crystal-like PTFE surface transferred by the rubbing technique indeed induced the orientation of the PVDF−TrFE crystals resulting from the epitaxy of two crystalline polymers in which *b* axis of PVDF−TrFE is matched with *a* axis of PTFE as schematically illustrated in Figure 3a. The permanent dipole between hydrogen and fluorine atom parallel

to *b* axis lies perpendicular to the surface normal. At the same time, the dipole can be oriented with the opposite direction with the same crystal ordering (Supporting Information, Figure S1). The orientation of the chain molecules in turn leads to microstructural ordering of the crystalline lamellae aligned perpendicular to the chain axis and at the same time to the rubbing direction of PTFE as depicted in Figure 3b. It should be noted that the perfect epitaxy illustrated in Figure 3a did not occur and there are some amounts of defects present in the sample due to not only conformational disorder arising from the random sequence of TrFE moiety in a chain but also the nonplanarity of both PTFE and PVDF−TrFE film as confirmed by the indication of weak (110).

The epitaxial orientation of PVDF−TrFE on the ordered PTFE surface allowed us not only to provide global orientation of the crystals but also, significantly, to remove the thermal hysteresis of ferroelectric polarization mainly arising from the alteration of the crystal orientation upon melting and recrystallization. The thermal hysteresis of PVDF−TrFE, observed at the first time in our recent work[10] and work by Li et al.,[33] involves the significant reduction of ferroelectric polarization during recrystallization following the crystal melting due to the rotation of *b* axis to the direction perpendicular to the electric field rendering electric field applied across the film in a capacitor the least effective. Although our effort to overcome the hysteresis is somewhat successful by an etched Al substrate with topographically textured periodic nanostructure in the temperature range limited to approximately 180 °C, [34] more improvement is in need for high temperature treatments frequently encountered in CMOS processes.

Since epitaxy is based on the crystallographic matching of two materials, crystal orientation is supposed to be maintained as long as the hosting substrate is preserved. In our system, high melting temperature of PTFE substrate (∼350 °C) in principle allows no thermal hysteresis of PVDF−TrFE up to 350 °C. Figure 4a shows the microstructure of PVDF−TrFE thin film heat-treated at 200 °C for 30 min on PTFE, following epitaxy at 135 °C. Regardless of the cooling rate to room temperature, the orientation induced by the eptiaxy still remains in spite of the presence of some more meandering crystalline lamellae (Figure 4a). In contrast, the characteristic in-plane lamellae with the *c* axis perpendicular to the surface are attributed to the crystal reorientation during heat treatment and are clearly observed on the bare SiO_2 surface not covered with PTFE as evidenced in the upper left region of Figure 4a. The SAD pattern of the heat treated sample also confirms the maintenance of the molecular orientation of PVDF−TrFE by the appearance of the spot-like reflection of $(001)_{PVDF-TrFE}$ parallel to $(0\ 0\ 15)_{PTFE}$ as shown in Figure 4b. The melting and recrystallization, however, slightly deteriorates the degree of epitaxy because the forbidden reflection of either (110) or (200) is apparent near 4.5 $Å^{-1}$ at the equator, leading to the meandering crystalline lamellae observed in Figure 4a.

In situ GIXD with a PVDF−TrFE sample on heating stage was very useful for investigating the evolution of crystal ordering upon melting and recrystallization. Both a thin PVDF−TrFE film epitaxially grown on PTFE surface and a film prepared on SiO_2 surface for comparison were slowly heated above T_m and cooled down to room temperature with the constant rate of 5 °C/min after heat treatment at 200 °C for 30 min. We monitored in particular the azimuthal intensity profile of reflection at the meridian because the peak at the meridian frequently disappeared due to the crystal rotation on a flat substrate during recrystallization. [10] Figure 4c shows the series of azimuthal intensity profiles near the meridian of *in situ* GIXD patterns of a PVDF−TrFE on PTFE captured during cooling process. No scattering from the molten PVDF−TrFE

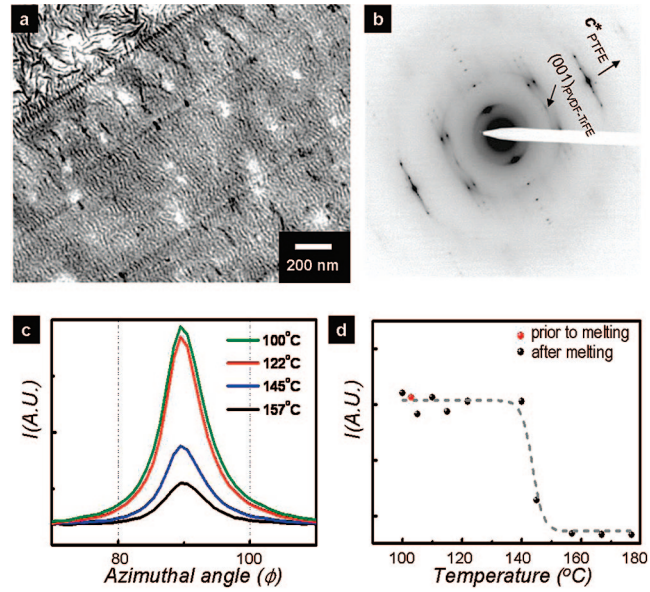

Figure 4. (a) Bright field TEM image of a PVDF−TrFE thin film epitaxially crystallized on PTFE surface followed by annealing at 200 °C and then subsequently cooled down to the room temperature. The ordered microstructure was maintained of crystalline lamellae of PVDF−TrFE aligned perpendicular to the rubbing direction of PTFE even after annealing process. (b) SAD pattern of crystalline structure corresponding to part a. (c) Azimuthal intensity profiles of (200) reflections collected at several temperatures from *in situ* GIXD patterns during the cooling from 200 °C to room temperature. The minimized intensity of reflected beam while the PVDF−TrFE crystals melt at 157 °C increased with the growth of crystals during the cooling process to the temperature of 100 °C. (d) Plot of the maximum intensity of (200) reflections as a function of various temperatures during heating and cooling cycle. With the melt and recrystallization, the intensity from (200) reflection recovers to the extent which the original sample prior to melting had.

was observed at the temperature above T_m with a trace of (010) reflection of PTFE crystals. Upon recrystallization of PVDF−TrFE near 145 °C, the intensity begins to appear and tends to increase with decreasing temperature as shown in Figure 4c. In contrast, the sample prepared on SiO_2 surface exhibited no intensity evolution of (110) reflection at the meridian during cooling due to the crystal rotation to the equator as previously reported. The maximum intensity at 90° of each profile was plotted as a function of temperature at which GIXD was captured during heating and cooling cycle in Figure 4d. It is apparent that the intensity at the temperature below T_m is almost similar to that at room temperature after one cycle without significant thermal hysteresis of (200) reflection, which implies that ferroelectric polarization of PVDF−TrFE film is preserved even after high temperature treatment with no requirement of additional electric poling. Our experimental data show that PVDF−TrFE crystal with HP structure is also oriented on PTFE surface at the temperature above its Curie point. The ordered HP crystals are transformed into LP ones with the crystal orientation maintained when the temperature is below its Curie point. Due to the larger (100) lattice of HP crystals (∼5.63 Å) than the (200) one of LP crystals (∼4.56 Å), the intensified (200) reflection of an epitaxially grown PVDF−TrFE film at the meridian appears at higher scattering vector, *q* at room temperature than at 140 °C as shown in Supporting Information Figure S2. Our results are somewhat different from those by Hua et al. where epitaxially grown HP crystals have been preserved even at low temperature regime due to the strong interaction with the graphite substrate which prevents the solid state crystal transition of PVDF−TrFE.[35] Our tolerant epitaxy even with approximately 7.2% lattice mismatch between *b* and *a* axis of PVDF−TrFE

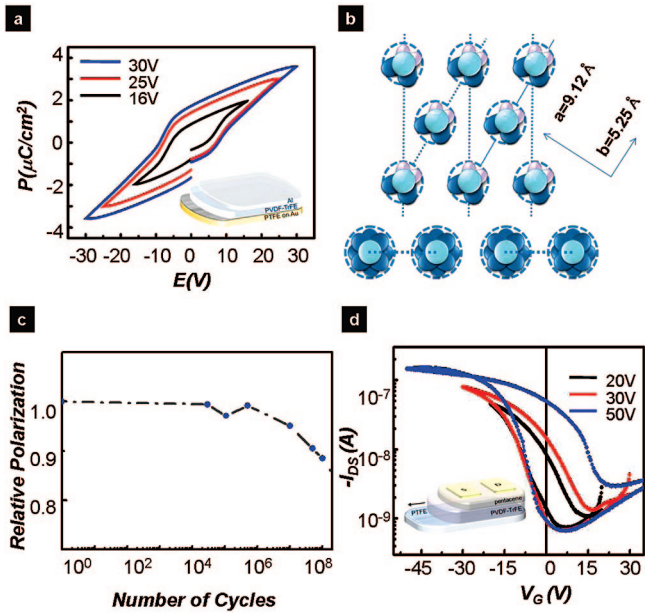

Figure 5. (a) Schematics of a capacitor structure with PVDF−TrFE thin film sandwiched between metal electrodes and polarization hysteresis loop with sweeping voltage applied. (b) Schematics of *bc* plane orientation of PVDF−TrFE crystal on PTFE substrate under electric field parallel to the surface normal of PTFE. (c) Normalized remanent polarization defined by the ratio of P_{rI} to P_{rN} as a function of number of cycles (N) in log scale, where of P_{rI} and P_{rN} correspond to the remanent polarization of initial state and a state after fatigue cycles of N, respectively. The fatigue properties were measured with frequency of 10^4Hz, and bipolar pulse train of ± 20 V. (d) Illustration of FeFET device structure and transfer characteristics of pentacene TFT with epitaxially grown PVDF−TrFE gate dielectric layer on PTFE substrate. The drain voltage V_D, channel length L, and width W are −5 V, 20 μm, and 200 μm, respectively.

and PTFE, respectively allowed the facile epitaxial solid state transition on PTFE surface.

A ferroelectric capacitor was easily fabricated by forming an ultra thin ca. 40 nm PVDF−TrFE thin film epitaxially grown on PTFE interlayer/bottom Au electrode and subsequently by depositing top Al electrode as shown in the schematic of Figure 5a. In our system, under the maximum voltage of ±30 V prior to electric breakdown of the PVDF−TrFE film, ferroelectric polarization switching occurred with relatively small remanent polarization of approximately 1.7 μC/cm^2 as shown in Figure 5a. Since approximately 30 nm thick PTFE interlayer has the dielectric constant (ε) of approximately 2.5 much lower than that of PVDF−TrFE layer ($\varepsilon \sim 10$), approximately 1/6 of the apparent applied voltage is exerted on PVDF−TrFE layer in the bilayered capacitor. Our capacitor seems to be therefore very efficient because it operates at the effective voltage exerted on PVDF−TrFE of approximately ±5 V. A control sample of 40 nm PVDF−TrFE spin coated and annealed on 30 nm thick poly(vinylphenol) (PVP) buffer layer did not exhibit ferroelectric polarization behavior with the similar effective voltage of ±5 V. We believe that the globally ordered PVDF−TrFE crystals on PTFE give rise to synchronized polarization switching, which renders the effective electric field applied to the sample significantly lowered. It is also noted that a 40 nm PVDF−TrFE film directly formed on a bottom electrode showed very large leakage current in most capacitors.

In fact, the molecular orientation of the crystalline PVDF−TrFE lamellae obtained by their epitaxy on PTFE is at glance not beneficial for effective ferroelectric polarization because the polar *b* axis is perpendicular to the electric field applied parallel to the surface normal of the film as shown in the schematic of Figure 3b. The pseudo hexagonal symmetry of crystal structure of PVDF−TrFE, however, allows the orientation shown in Figure 3b to be transformed into one in Figure 5b with ease by rotating the H−F dipole under electric field. Our previous work demonstrated that the rotation of the dipole required only the slightly higher electric field at the beginning, leading to the final remanent polarization very similar to that obtained from a sample with the crystal structure not necessary for the rotation. The maximum polarization that can be obtained with the crystal orientation in Figure 5b is 87% of the ideal polarization of PVDF−TrFE crystals whose *b* axis is completely parallel to the electric field. Due to H−F dipole symmetry, it is also possible to have another orientation in PVDF−TrFE as schematically illustrated in Supporting Information Figure S3.

The globally ordered microstructure of PVDF−TrFE can certainly improve the property of repeated switching on polarization, i.e, fatigue due to the collective and synchronized dipole switching resulting from much fewer structural defects.[36] We examined fatigue properties by applying bipolar switching pulse train in the capacitor structure. Figure 5c demonstrates the normalized remanent polarization as a function of number of cycles, N, when the polarization was obtained with driving voltage of ±20 V and fatigue stress frequency, f of 10 000 Hz. With the switching stress proceeding to approximately 10^6 cycles, normalized remanent polarization is preserved. The polarization gradually decreases to 88.5% of the initial value after the itinerant stress cycles of 5×10^8. Our results with ca. 40 nm thick film is very comparable with those reported by Zhu et al. in 1 μm thick PVDF−TrFE copolymer films.[37] Since the polarization loss by fatigue follows a universal scaling behavior with N/f, the 12% reduction of our sample at 5×10^4 is remarkable, compared with approximately 20% loss of polarization reported under the similar electric field applied of approximately 85 MV/m.[37]

The relatively low remament polarization of 1.7 μC/cm^2 of our oriented PVDF−TrFE on PTFE is sufficiently large to operate a FeFET in which a ferroelectric film is used as a gate dielectric. The fact that a low P_r of approximately 2 μC/cm^2 is required for Si based FeFET memory renders our method potentially more suitable for FeFET memory.[38] An epitaxially grown PVDF−TrFE thin film was prepared on Au gate electrode coated with PTFE thin film on which pentacene thin layer and Au source/drain electrodes were sequentially deposited as schematically illustrated in Figure 5d. The device clearly shows typical source/drain current hysteresis curves as a function of the gate sweep voltage. The hysteresis was saturated with ON/OFF bistability of 10^2 at the gate sweep voltage of 50 V arising from ferroelectric polarization switching of the PVDF−TrFE gate dielectric.

Conclusion

High throughput epitaxy of a thin ferroelectric PVDF−TrFE film based on spin coating technique was developed with molecularly ordered PTFE substrate. The crystallographic lattice match between two polymers (a_{PTFE} // $b_{PVDF-TrFE}$) produced nearly single crystal texture of PVDF−TrFE thin film whose *bc* plane was preferentially contacted with *ac* one of PTFE, resulting in the edge-on PVDF−TrFE crystalline lamellae aligned perpendicular to the rubbing direction of PTFE, its *c*-axis. Large area epitaxy enabled us not only to minimize the thermal hysteresis of crystal orientation but also to fabricate the arrays of 200 μm metal/ferroelectric polymer/metal capacitors exhibiting the efficient polarization switching at the effective operation voltage of ±5 V and with the 88% of preserved polarization after the fatigue test of applying bipolar switching pulse with 5×10^8 cycles. Also, a FeFET memory including epitaxially grown PVDF−TrFE film as gate dielectric confirmed bistable $I-V$ characteristic arising from ferroelectric polarization.

Acknowledgment. This project was supported by The National Research Program for the 0.1 Terabit Non-Volatile Memory Development and "SYSTEM2010" project sponsored by Korea Ministry of Knowledge, Economy and Samsung Electronics, Co., Ltd. The X-ray experiments at PAL (4C2 beamline), Korea, were supported by MOST and POSCO, Korea. We also thank ESRF for providing a FIT 2D software. This work was supported by the Second Stage of Brain Korea 21 Project in 2008, Seoul Science Fellowship, the Korea Research Foundation Grant funded by the Korean Government (MOEHRD) (KRF-2006-612-D00027), and the Korea Science and Engineering Foundation (KOSEF) grant funded by the Korea government (MEST) (No. R11-2007-050-03001-0).

Supporting Information Available: Figures showing illustration of molecular orientation of PVDF-TrFE thin film, 2D GIXD patterns of PVDF−TrFE/PTFE bilayered films, and the illustration of the *bc* plane of PVDF−TrFE crystals. This material is available free of charge via the Internet at http://pubs.acs.org.

References and Notes

(1) Ducharme, S.; Reece, T. J.; Othon, M. C.; Rannow, R. K. *IEEE Trans. Device Mater. Reliab.* **2000**, *5*, 720.
(2) Naber, R. C. G.; Tanase, C.; Blom, P. W. M.; Gelinck, G. H.; Marsman, A. W.; Touwslager, F. J.; Setayesh, S.; De Leeuw, D. M. *Nat. Mater.* **2005**, *4*, 243.
(3) Gelinck, G. H.; Marsman, A. W.; Touwslager, F. J.; Setayesh, S.; De Leeuw, D. M.; Naber, R. C. G.; Blom, P. W. M. *Appl. Phys. Lett.* **2005**, *87*, 092903.
(4) Lovinger, A. J. *Science* **1983**, *220*, 1116.
(5) Fujisaki, S.; Ishiwara, H.; Fujisaki, Y. *Appl. Phys. Lett.* **2007**, *90*, 162902.
(6) Kang, S. J.; Park, Y. J.; Park, C.; Sung, J.; Jo, P. S.; Kim, K. J.; Cho, B. O. *Appl. Phys. Lett.* **2008**, *92*, 012921.
(7) Naber, R. C. G.; Blom, P. W. M.; Marsman, A. W.; De Leeuw, D. M. *Appl. Phys. Lett.* **2004**, *85*, 2032.
(8) Zhang, Q. M.; Xu, H.; Fang, F.; Cheng, Z.-Y.; You, H. *J. Appl. Phys.* **2001**, *89*, 2613.
(9) Xia, F.; Xu, H. H.; Razavi, B.; Cheng, Z.-Y.; Zhang, Q. M *J. Appl. Phys.* **2002**, *92*, 3111.
(10) Park, Y. J.; Kang, S. J.; Park, C.; Kim, K. J.; Lee, H. S.; Lee, M. S.; Chung, U. -I.; Park, I. J. *Appl. Phys. Lett.* **2006**, *88*, 242908.
(11) Park, Y. J.; Kang, S. J.; Lotz, B.; Thierry, A.; Kim, K. J.; Huh, J.; Park, C. *Macromolecules* **2008**, *41*, 109.
(12) Petermann, J.; Gohil, R. M. *J. Mat. Sci.* **1979**, *14*, 2260.
(13) Yang, D. C.; Thomas, E. L. *J. Mater. Sci.* **1984**, *3*, 929.
(14) Yang, D. C.; Thomas, E. L. *J. Mater. Sci. Lett.* **1987**, *6*, 593.
(15) Kaufmann, W.; Petermann, J.; Reynolds, N.; Thomas, E. L.; Hsu, S. L. *Polymer* **1989**, *30*, 2147.
(16) Matsushige, K.; Nagata, K.; Imada, S.; Takemura, T. *Polymer* **1980**, *21*, 1391.
(17) Wang, T. T. *J. Appl. Phys.* **1979**, *50*, 6091.
(18) Kang, S. J.; Park, Y. J.; Hwang, J.; Jeong, H. J; Lee, J. S.; Kim, K. J.; Kim, H.-C.; Huh, J.; Park, C. *Adv. Mater.* **2007**, *19*, 581.
(19) Anderson, P. S.; Guerin, S.; Hayden, B. E.; Khan, M. A.; Bell, A. J.; Han, Y.; Pasha, M.; Whittle, K. R.; Reaney, I. M. *Appl. Phys. Lett.* **2007**, *90*, 202907.
(20) Fuflyigin, V.; Osinsky, A.; Wang, F.; Vakhutinsky, P.; Norris, P. *Appl. Phys. Lett.* **2000**, *76*, 1612.
(21) Theis, C. D.; Yeh, J.; Schlom, D. G.; Hawley, M. E.; Brown, G. W. *Thin Solid Films* **1998**, *325*, 107.
(22) Lin, Y.; Zhao, B. R.; Peng, H. B.; Hao, Z.; Xu, B.; Zhao, Z. X.; Chen, J. S. *J. Appl. Phys.* **1999**, *86*, 4467.
(23) Wittman, J. C.; Lotz, B. *J. Polym. Sci., Polym. Phys. Ed.* **1981**, *19*, 1837.
(24) Wittman, J. C.; Lotz, B. *Prog. Polym. Sci.* **1990**, *15*, 909.
(25) De Rosa, C.; Park, C.; Lotz, B.; Thomas, E. L. *Nature* **2000**, *405*, 433.
(26) Wittmann, J. C.; Smith, P. *Nature* **1991**, *352*, 414.
(27) Amundson, K. R.; Sapjeta, B. J.; Lovinger, A. J.; Bao, Z. *Thin Solid Films* **2002**, *414*, 143.
(28) Sirringhaus, H.; Brown, P. J.; Friend, R. H.; Nielsen, M. M.; Bechgaard, K.; Langeveld-Voss, B. M. W.; Spiering, A. J. H.; Janssen, R. A. J.; Meijer, E. W.; Herwig, P.; de Leeuw, D. M. *Nature* **1999**, *401*, 685.
(29) Tashiro, K.; Tanaka, R. *Polymer* **2006**, *47*, 5433.
(30) Wang, Z.; Fan, H.-Q.; Su, K.-H.; Wang X.; Wen, Z.-Y *Polymer* **2007**, *48*, 3226.
(31) Yamada, T.; Ueda, T.; Kitayama, T. *J. Appl. Phys.* **1981**, *52*, 948.
(32) Diffraction of the Cerius^2 package developed by Accelrys.
(33) Zhang, L.; Ducharm, S.; Li, J. *Appl. Phys. Lett.* **2007**, *91*, 172906.
(34) Park, Y. J.; Kang, S. J.; Park, C; Woo, E.; Shin, K.; Kim, K. J *Appl. Phys. Lett.* **2007**, *90*, 222903.
(35) Hua, T.-T.; Itoh, T.; Fugiwara, S.; Hashimoto, M. *J. Phys. Soc. Jpn.* **2007**, *76*, 124604.
(36) Scott, J. F. *Ferroelectric Memories*; Springer: Heidelberg, Germany, 2000, Chapter 7.
(37) Zhu, G.; Zeng, Z.; Zhang, L.; Yan, X. *Appl. Phys. Lett.* **2006**, *89*, 102905.
(38) Setter, N.; Damjanovic, D.; Eng, L.; Fox, G.; Gevorgian, S.; Hong, S.; Kingon, A.; Kohlstedt, H.; Park, N. Y.; Stephenson, G. B.; Stolitchnov, I.; Taganstev, A K.; Taylor, D. V.; Yamada, T.; Streiffer, S *J. Appl. Phys.* **2006**, *100*, 051606.

MA801495K